2014 IEEE International Conference on Robotics & Automation (ICRA)
Hong Kong Convention and Exhibition Center
May 31 - June 7, 2014. Hong Kong, China

Cartesian-Space Control and Dextrous Manipulation for Multi-Fingered Tendon-Driven Hand

Taylor Niehues, Julia Badger, Myron Diftler, Ashish D. Deshpande

Abstract— **Dextrous object manipulation is a crucial task for the hands of the space humanoid Robonaut 2 (R2), and requires accurate control of fingertip positions and forces. We present a novel Cartesian control for the fingers and thumb of the R2 hand. The controller is designed such that the singularities in the fingers are avoided, and distal joint stiffness is added in the thumb for full controllability. We then present a higher-level object stiffness control law for explicit control of object position, orientation, and grasp forces. The complete algorithm is tested experimentally on the R2 hand, with results demonstrating tracking performance and robustness against disturbances.**

I. Introduction

Manipulating objects dextrously with a robotic hand is challenging. A number of approaches have been explored to achieve object manipulation, but this still is an open research problem [1], [2], [3]. Our goal is to realize object manipulation with the hand system of the space humanoid, Robonaut 2 (Fig. 1).

Since contact with the fingertips is prominent during many fine manipulation tasks, precise control of fingertip positions and forces is critical. Cartesian stiffness control is a strategy that implements a user-defined fingertip stiffness, creating a linear force/position relationship in quasi-static situations [4]. For dynamic interactions, a Cartesian impedance controller gives the fingertips a user-defined mechanical impedance as it interacts with the environment [5]. Cartesian impedance control has previously been implemented successfully in robotic fingers, such as in the DLR Hand II [6]. From a design perspective, tendon-driven actuation in robotic hands results in lower finger inertias, a desirable trait, but also presents the challenge of simultaneously controlling multiple tendons.

The hands of the Robonaut 2 (R2) are designed to achieve human-like grasping and manipulation in an unstructured environment, such as the International Space Station (ISS) [7]. The fingers and thumbs are tendon-driven to allow for remote actuation and reduced finger size and weight. The primary (index and middle) fingers and the thumbs each have $n+1$ tendons for n joints, which leads to full finger controllability ($n = 3$ for primary fingers and $n = 4$ for thumbs). While this "$n + 1$" tendon arrangement is attractive due to the low actuator count and space requirement, it also results in a complex control problem, especially for impedance control. Thus far, a joint-space torque control law for the individual R2 fingers has been developed [8] that solves the tendon tension distribution problem and produces decoupled motions in the joint-space. However, Cartesian control of the fingertips has not yet been explored.

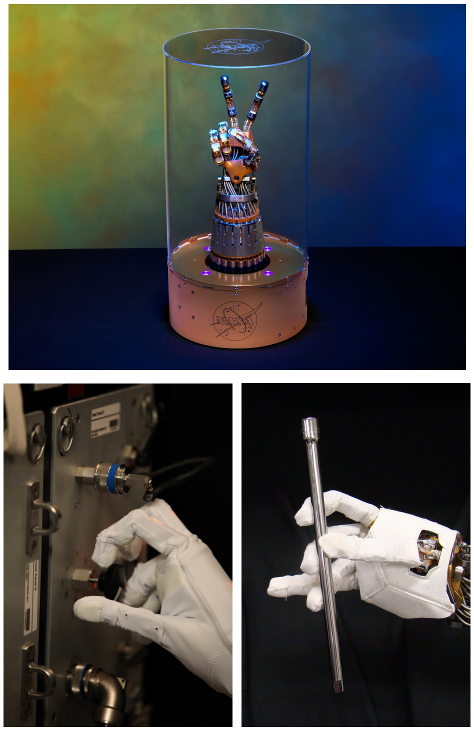

Fig. 1. The Robonaut 2 (R2) upper body system and examples of the challenging manipulation tasks to be performed by the R2 hands on the International Space Station.

Once Cartesian control of the fingers is achieved, the next challenge is to implement a higher-level coordinated controller for object manipulation. This involves simultaneous control of multiple fingers. In the past, the R2 hands accomplished grasping and manipulation tasks by generating finger joint trajectories specifically for a given object. This method requires complex path planning, and makes it difficult to control contact forces. Here we present an *object-level control* strategy which allows for better control of grasp forces while avoiding both contact slippage and unnecessarily high internal forces, and also gives us direct control of object position without explicit finger position commands. In addition, we use an object stiffness law to

This work was supported, in part, by the National Science Foundation (grant # 1157954).

Taylor Niehues and Ashish D. Deshpande are with the Department of Mechanical Engineering, The University of Texas at Austin, Austin, Texas 78712, USA taylor.niehues@utexas.edu, ashish@austin.utexas.edu

Julia Badger and Myron Diftler are with the Johnson Space Center, NASA, Houston, TX 77058, USA {julia.m.badger, myron.a.diftler}@nasa.gov

978-1-4799-3684-7/14/$31.00 ©2014 IEEE

provide safer environmental interactions and user-definable stiffness properties in each Cartesian direction.

Previously, Lee et al. [9] used object stiffness control to create a relationship between positions and forces in the object frame for planar, tendon-driven fingers. Simulation studies in [10], [11] present a control law for two-fingered pinching grasps with rolling contacts, applied to both 2-D and 3-D cases. Gabiccini et al. [12] used an algorithm that integrates a computed torque law for three anthropomorphically designed tendon-driven fingers grasping an object by optimizing the tendon actuation to meet tension constraints. An object impedance control strategy, as presented by Schneider and Cannon [13], allows for control of the impedance behavior of the object using a grasp matrix mapping. Prattichizzo [14] and Malvezzi [15] developed an object-motion decoupled internal force controller to reduce the effect of internal forces on object trajectory. Manipulation experiments with an object impedance controller have been performed for the DLR Hand II [16], [17] using direct-drive joints and joint torque measurements. However, object manipulation experiments have not been presented for the tendon-driven DLR Hand-Arm System [2], a more difficult control problem due to its complex tendon arrangement.

In this paper we present a Cartesian stiffness control algorithm for the individual R2 fingers and thumbs and an object-level stiffness controller for fine manipulation tasks. We chose a Cartesian stiffness controller over an impedance controller because damping and inertia are not significant in our control problem. It has been shown for the R2 finger control that the parameters in the joint torque controller can be easily tuned to produce a critically damped response [8], which eliminates the need for damping controls. Also, the finger inertias are small enough that inertia shaping is not necessary [7]. In the finger Cartesian controllers, necessary modifications are made based on the R2 finger kinematics (e.g. singularity avoidance), and force feedback is provided solely by tendon tension sensors. The object-level stiffness controller allows for explicit control of grasp forces and object position and orientation, and is robust against impacts and other disturbances and uncertainties. The complete algorithm is tested experimentally on the R2 hand.

II. Finger Controller

We first design a Cartesian controller for the individual R2 fingers and thumbs. This problem is divided into two smaller control tasks: control of finger joint torques through tension feedback, and implementation of a Cartesian stiffness controller for regulation of both fingertip positions and forces. Variables used can be found in Table I.

A. Joint Torque Controller

To control the finger joint torques, we use the joint-space controller proposed in [8]. The actual joint torques $\boldsymbol{\tau}$ and internal tension t can be found using sensed tension values, $\mathbf{f}_\ell$, through the relation:

$$\bar{\boldsymbol{\tau}} = \begin{bmatrix} \boldsymbol{\tau} \\ t \end{bmatrix} = P\mathbf{f}_\ell \tag{1}$$

where $P \in \mathbb{R}^{(n+1)\times(n+1)}$ is the tendon map matrix, which contains the joint radii data to map from tendon tensions to joint torques, as well as the null-space component of tension combinations that produce zero net joint torque.

TABLE I

Description of variables.

Variable	Description
$\boldsymbol{\ell} \in \mathbb{R}^{(n+1)}$	motor positions
$\mathbf{f}_\ell \in \mathbb{R}^{(n+1)}$	tendon tensions
$\mathbf{q} \in \mathbb{R}^{n}$	joint positions
$\boldsymbol{\tau} \in \mathbb{R}^{n}$	joint torques
$\mathbf{x} \in \mathbb{R}^{3}$	fingertip Cartesian position
$\mathbf{f}_x \in \mathbb{R}^{3}$	fingertip Cartesian forces
$J(\mathbf{q}) \in \mathbb{R}^{3\times n}$	Jacobian matrix of finger
$W(\mathbf{x}) \in \mathbb{R}^{3\times 6}$	grasp matrix

The actuators already employ well-tuned PD position control loops, so the torque control loop should pass down desired actuator positions $\boldsymbol{\ell}_d$ to the motor controllers. Given an initial set of desired joint torques $\boldsymbol{\tau}_{d,init}$, the internal tension t_d can be found using a tension distribution algorithm such that each commanded tension is within a bounded range $[f_{min}, f_{max}]$. To ensure the tension bounds hold, we linearly scale the torques such that:

$$\boldsymbol{f}_\ell = P^{-1} \begin{bmatrix} \alpha\boldsymbol{\tau}_{d,init} \\ t_d \end{bmatrix} = P^{-1}\bar{\boldsymbol{\tau}}_d \tag{2}$$

where α is a positive scalar in the range $(0, 1]$. The solution to this tension distribution algorithm (see [8]) produces a combined desired joint torque and internal tension, $\bar{\boldsymbol{\tau}}_d$, that ensures bounded tendon tensions $\mathbf{f}_\ell \in [f_{min}, f_{max}]$.

Then, the joint-space controller is defined as

$$\boldsymbol{\ell}_d = \boldsymbol{\ell} - k_d\dot{\boldsymbol{\ell}} + P^T K_p(\bar{\boldsymbol{\tau}}_d - \bar{\boldsymbol{\tau}}) \tag{3}$$

where k_d is a scalar damping gain and $K_p \in \mathbb{R}^{(n+1)\times(n+1)}$ is a diagonal matrix containing torque and internal tension proportional gains.

B. Cartesian Stiffness Controller

For accurate control of fingertip positions and forces, we would like to produce a fingertip Cartesian stiffness of the form:

$$\mathbf{f}_{x,d} = K_x(\mathbf{x}_d - \mathbf{x}) \tag{4}$$

where the fingertip position $\mathbf{x}$ is calculated from the joint angles $\mathbf{q}$ using the forward kinematics. From a desired fingertip force, we can find the desired joint torques by applying the transformation

$$\boldsymbol{\tau}_d = J(\mathbf{q})^T\mathbf{f}_{x,d} = J(\mathbf{q})^T K_x(\mathbf{x}_d - \mathbf{x}) \tag{5}$$

This defined stiffness is the foundation of the finger Cartesian controllers, but it is slightly modified to fit specifically with the R2 thumb and primary finger kinematics. The secondary ring and little fingers are both underactuated (3 tendons to control 4 DOFs), and thus are not fully controllable in Cartesian-space.

1) Thumb: In the case of the thumb, simply using the Jacobian $J(\mathbf{q}) \in \mathbb{R}^{3\times4}$ to transform from 3-D Cartesian forces to four joint torques leaves one uncontrolled internal DOF. To address this, we explicitly control the thumb's distal joint angle q_4 with a desired joint stiffness. Control of the distal joint angle is useful during grasping and manipulation tasks, allowing us to ensure that contact is being made with the flat pad of the thumb for a more stable grasp. This results in a new joint torque formulation,

$$\boldsymbol{\tau}_d = \begin{bmatrix} (J_{3\times3})^T K_{x,thumb}(\mathbf{x}_d - \mathbf{x}) \\ k_{dist}(q_{4d} - q_4) \end{bmatrix} \tag{6}$$

where $J_{3\times3}$ is the thumb Jacobian $J(\mathbf{q})$ with the last column removed, and k_{dist} is the desired distal joint stiffness.

2) Primary Fingers: In the primary fingers, a singular position occurs when the fingertip is aligned with the proximal yaw joint axis. At this singularity, movement of the yaw joint produces zero change in the fingertip Cartesian position, meaning the finger cannot produce lateral motions or forces. Because the finger frequently moves through this singular position and the yaw joint is already relatively ill-conditioned due to its smaller joint radii, the controller tends to performs poorly near this singularity. Therefore, we switched from Cartesian control of lateral abduction/adduction finger motions to joint stiffness control of the yaw joint q_1, such that

$$\boldsymbol{\tau}_d = \begin{bmatrix} 1 & 0 \quad 0 \\ 0 & \\ 0 & (J_{2\times2})^T \end{bmatrix} K_{x,prim} \begin{bmatrix} q_{1d} - q_1 \\ y_d - y \\ z_d - z \end{bmatrix} \tag{7}$$

where $K_{x,prim}$ = diag(k_{yaw}, k_y, k_z) is the new stiffness gain matrix for primary fingers and $J_{2\times2}$ is the primary finger Jacobian $J(\mathbf{q})$ after removing the column representing the yaw joint and the row representing the lateral Cartesian direction. Using this reduced Jacobian, we will only specify a Cartesian stiffness in two directions: the z-direction defined as being orthogonal to the plane of the palm, and the y-direction defined as being parallel to the plane of the palm and orthogonal to the proximal flexion/extension joint axis.

This produces more stable and controllable motions throughout the finger's range of motion without hampering our ability to control fingertip Cartesian position and force, due to the simplicity of transforming from lateral position/force to yaw joint angle/torque, and vice versa. Control of the yaw joint also helps us more effectively manage the location of the point of contact on the finger's surface during environmental interactions, i.e. to avoid grasping an object with the side of a finger.

To avoid singularity positions and to avoid hitting mechanical hard stops at the joint limits, repelling torques are used at each finger joint:

$$\tau_{lim,i} = \begin{cases} -k_i[q_i - (q_{i,max} - \delta_i)], & \text{for } q_i > q_{i,max} - \delta_i \\ k_i[q_i - (q_{i,min} + \delta_i)], & \text{for } q_i < q_{i,min} + \delta_i \\ 0 & \text{otherwise} \end{cases} \tag{8}$$

where $q_{i,min}$, $q_{i,max}$ are the joint limits, δ_i is the desired safe distance, and k_i is the repelling stiffness. This repelling torque is added to the joint torques of the Cartesian controller.

The total desired torques $\boldsymbol{\tau}_d$ calculated here will be passed down to the joint-space controller in Sec. II-A. The gains K_p and k_d in Eq. (3) are tuned to give the Cartesian stiffness controller a critically damped step response.

III. Object Manipulation Controller

The goal of the object manipulation controller is to robustly grasp and manipulate an object using the thumb and two primary fingers. It is designed to produce 2-D motions on a plane parallel to the palm of the hand.

We first define a stiffness force to be applied to the object.

$$\mathbf{f}_{obj} = \begin{bmatrix} f_x \\ f_y \\ \tau \end{bmatrix}_{obj} = K_{obj} \begin{bmatrix} x_{od} - x_o \\ y_{od} - y_o \\ \phi_d - \phi \end{bmatrix} \tag{9}$$

where K_{obj} is a diagonal object stiffness matrix, the object position (x_o, y_o) is defined as the centroid of the three fingertip positions, and the object angle ϕ is defined as the angle between the object position and thumb. The combination of (x_o, y_o, ϕ) defines the object's virtual position.

To find the desired fingertip forces, we use the following relation:

$$\mathbf{f}_{obj} = W(\mathbf{x})\mathbf{f}_c \tag{10}$$

where $W(\mathbf{x})$ is the grasp matrix and $\mathbf{f}_c \in \mathbb{R}^6$ represents the 2-D contact forces at each of the three fingertips.

Finding the inverse relation requires the generalized pseudoinverse $W^+(\mathbf{x})$, along with the null-space matrix $N(\mathbf{x})$ containing the internal forces. Simply calculating the null-space of $W(\mathbf{x})$ results in $N(\mathbf{x}) \in \mathbb{R}^{6\times3}$, which would require controller optimization of three separate internal force variables. To reduce the null-space, we introduce an additional constraint that the line of action of the internal forces must pass through the object's center. These internal forces would act in the same directions as those produced by the passivity-based object controller of Wimboeck et. al. [16], which uses virtual springs connecting each fingertip to the center of the object. For more complex object shapes, different constraints may be chosen by the user depending on geometry and task requirements.

For example, a constraint for the thumb would be:

$$\begin{gathered} \frac{f_{t,y}}{f_{t,x}} = \frac{y_t - y_o}{x_t - x_o} \\ (y_t - y_o)f_{t,x} - (x_t - x_o)f_{t,y} = C_1(\mathbf{x})\mathbf{f}_c = 0 \end{gathered} \tag{11}$$

where $C_1(\mathbf{x}) \in \mathbb{R}^{1\times6}$ is a constraint row vector. In the same way, we set up a similar constraint row vector $C_2(\mathbf{x})$ for either one of the primary fingers, such that $C_2(\mathbf{x})\mathbf{f}_c = 0$. Now we can reduce $N(\mathbf{x})$ to a null-space column vector $\mathbf{n}(\mathbf{x}) \in \mathbb{R}^6$:

$$\mathbf{n}(\mathbf{x}) = nullspace\left(\begin{bmatrix} W(\mathbf{x}) \\ C_1(\mathbf{x}) \\ C_2(\mathbf{x}) \end{bmatrix}\right) \tag{12}$$

This definition of the null-space ensures that forces acting in the space of $\mathbf{n}(\mathbf{x})$ produce zero net object forces or torques

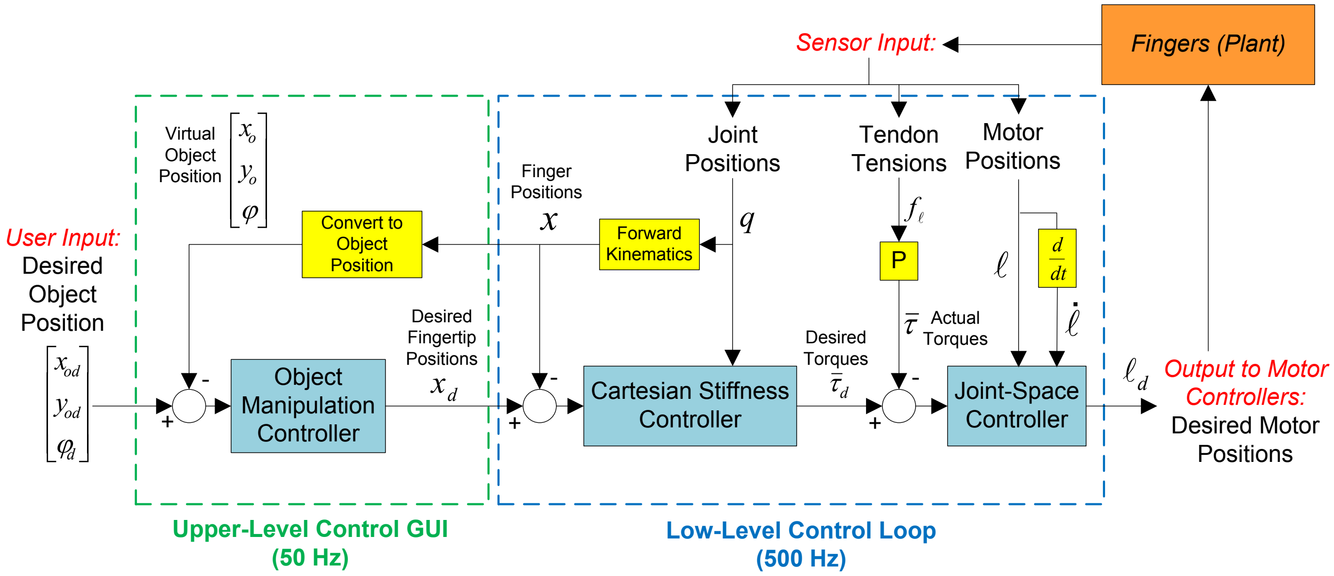

Fig. 2. Block diagram for the complete control system, including the high-level object stiffness controller and the low-level finger Cartesian stiffness and joint-space torque controllers. Note that the finger positions $\mathbf{x}$ and $\mathbf{x}_d$ include the primary finger yaw joint (q_1) and thumb distal joint (q_4) angles to be used by the Cartesian controllers.

and also realize the two constraint equations, such that the internal force vector will only produce forces passing through the object's center. Now, we can define the inverse relation:

$$\mathbf{f}_c = W^+(\mathbf{x})\mathbf{f}_{obj} + \mathbf{n}(\mathbf{x})\lambda \tag{13}$$

The internal force component, λ, is calculated such that the minimum normal force being produced at the three fingertips is greater than some prescribed minimum force $f_{grip,min}$.

The desired contact forces $\mathbf{f}_c$ are then converted into desired fingertip positions using Eq. (4) for the each finger's Cartesian control loop. For example, given a desired endpoint force $f_{x,ij}$ for finger i in the Cartesian direction j, the desired Cartesian position $x_{d,ij}$ is found as:

$$x_{d,ij} = x_{ij} + \frac{f_{x,ij}}{k_{x,ij}} \tag{14}$$

where $k_{x,ij}$ is the Cartesian stiffness for that particular finger and direction. The desired position $\mathbf{x}_d$ for each finger will be passed down to the corresponding Cartesian controller in Sec. II-B.

For the thumb, the commanded distal joint position q_{4d} is set to an angle ideal for maximum contact area on the thumb pad. For the primary fingers, the total torque required at the base to produce the desired fingertip force would be

$$\boldsymbol{\tau}_d = \mathbf{r} \times \mathbf{f}_{x,d} \tag{15}$$

where $\mathbf{r}$ is the vector from the finger base to the fingertip. Projecting $\boldsymbol{\tau}_d$ onto the yaw joint axis yields the desired yaw torque $\tau_{yaw,d}$. Then, the desired yaw angle is found as

$$q_{1d} = q_1 + \frac{\tau_{yaw,d}}{k_{yaw}} \tag{16}$$

and passed down to the Cartesian controller. The ability to control the yaw angle explicitly proves to be an important feature to ensure that the three finger contact points remain sufficiently spread out to maintain a quality force-closure grasp. The fingertip positions are also modified for stability purposes. For example, the internal force component is not allowed to drive the commanded fingertip positions past the object's center, so that if the object slips or is dropped, the fingers will simply come together and stop.

The higher-level object manipulation controller will pass down commanded Cartesian positions $\mathbf{x}_d$, primary yaw joint angles q_{1d}, and thumb distal joint angles q_{4d} to the finger Cartesian stiffness controllers.

IV. Experimental Manipulation Results

The object manipulation controller is implemented on the Robonaut 2 hand. A diagram illustrating the overall control structure is found in Fig. 2. Individual finger Cartesian controllers, combined with joint-space controllers to determine output motor positions, are implemented in a lower-level control loop communicating with the motor controllers at a rate of 500 Hz. The higher-level object manipulation controller runs on a separate computer running the R2 control GUI, which sends finger position commands down to the low-level controller at a rate of 50 Hz.

This relatively slow communication rate would result in instability without the inherent stability provided by the lower-level finger Cartesian controllers. This communication hierarchy shows a structure similar to human hand neuromuscular control: the communication rate of neural signals between the brain and the hand is slow (<10 Hz [18]), but the inherent stability and stiffness properties of the individual fingers (due to muscles, tendons, ligaments, joint capsules, etc.) allow robust manipulation abilities.

The control law is evaluated using a step rotation command about the object's z-axis and step commands in the

TABLE II

CONTROLLER PARAMETERS (UNITS ARE MM, RAD, AND TENSION SENSOR FORCE UNITS).

Parameter	Value
Primary Finger Stiffness	
$K_{x,prim}$	$= diag(k_{yaw}, k_y, k_z) = diag(1000, 0.05, 0.1)$
Thumb Stiffness	
$K_{x,thumb}$	$= diag(k_x, k_y, k_z) = diag(0.05, 0.05, 0.1)$
k_{dist}	250
Step Response Object Controller Parameters	
K_{obj}	$= diag(k_x, k_y, k_\phi) = diag(2.0, 2.0, 1500)$
$f_{grip,min}$	0.2
Disturbance Response Object Controller Parameters	
K_{obj}	$= diag(k_x, k_y, k_\phi) = diag(0.5, 0.5, 1000)$
$f_{grip,min}$	0.5

x and y translational directions. In addition, disturbance rejection experiments are performed to test the controller's robustness and ensure the desired object stiffness is being produced. For all cases, the desired object height above the palm is set to a constant value, such that the finger and object motions remain in a 2-D plane parallel to the palm. The object is a standard 0.04 kg racquetball with a radius of 57 mm.

By using a simple ball as an object, the grasp matrix can be easily approximated; for more complex object geometries, analysis may be needed to define a suitable virtual object frame and to define internal force constraints that work to keep the contact forces within their respective friction cones. For these experiments, the object's position shown in plots is its virtual position. Recording the actual position of the ball, i.e. through a motion capture system, will be part of future work to confirm controller performance.

The joint-space torque feedback gain K_p in Eq. (3) is determined experimentally for each finger to produce accurate joint torque tracking and internal tension maintenance; slight variations in K_p between the R2 fingers is necessary primarily due to tension sensor calibration errors. The damping gain k_d is set to 0.01. The remaining controller parameters used in the experiments can be found in Table II. The prescribed finger stiffness in the z-direction is larger than in other directions to help maintain the fingertips' positions on a fixed 2-D plane above the palm.

A. Object Rotation

The object is rotated about the z-axis by giving a step input of $\Delta\phi = -1.0\ rad$ (Fig. 3). The steady-state error in object angle and x occurs because the primary fingers both reach their yaw joint angle limits, causing the controller to compromise between the errors in x and object angle.

B. Object Translation

We perform object translation in the x-direction (laterally) by commanding a step input from from $x = -10\ mm$ to $x = -25\ mm$ (see Fig. 4), where the point $(x, y) = (0, 0)$ is located at the base of the middle finger. We once again see steady-state errors in x and object angle due to the primary fingers reaching their yaw joint limits.

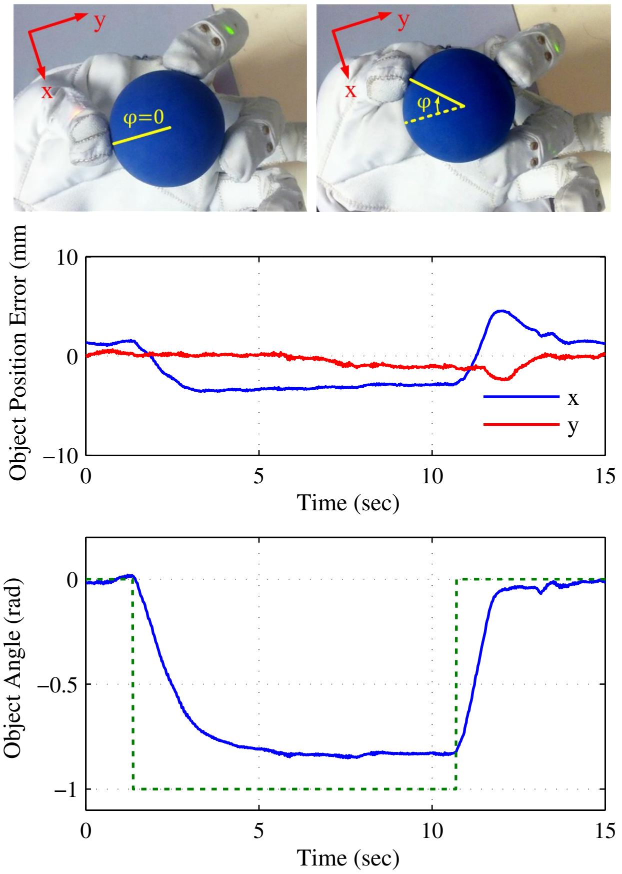

Fig. 3. The R2 hand rotating a ball about the z-axis, given a commanded object angle step input of $\Delta\phi = -1.0\ rad$.

Next, we test a step command in the y-direction of $y = 10\ mm$ to $y = -30\ mm$, as shown in Fig. 5. We see minimal errors in x or object angle, and negligible steady-state error in y. The slower rise time moving in the positive y-direction is a result of the thumb overcoming the grip forces being applied the two primary fingers, which must remain fairly high to maintain contact without slipping.

C. Disturbance Response

The disturbance response is analyzed to show the robustness of the controller. An external force is applied to the object, as shown in Fig. 6, and the resulting position and tendon tensions were recorded. The advantages of this object stiffness controller over a more straightforward position controller is the ability to react to disturbances and continuously modify the fingertip forces to maintain a stable grasp. Note that the controller parameters were adjusted (see Table II) for a lower object stiffness and higher internal forces to give clearer experimental results and reduce contact point slippage. The algorithm is able to maintain the desired posture effectively with an acceptable steady-state error.

The forces being applied to the object, calculated from the recorded tendon tensions and shown in Fig. 6(c), correspond approximately to the desired object stiffness. The internal

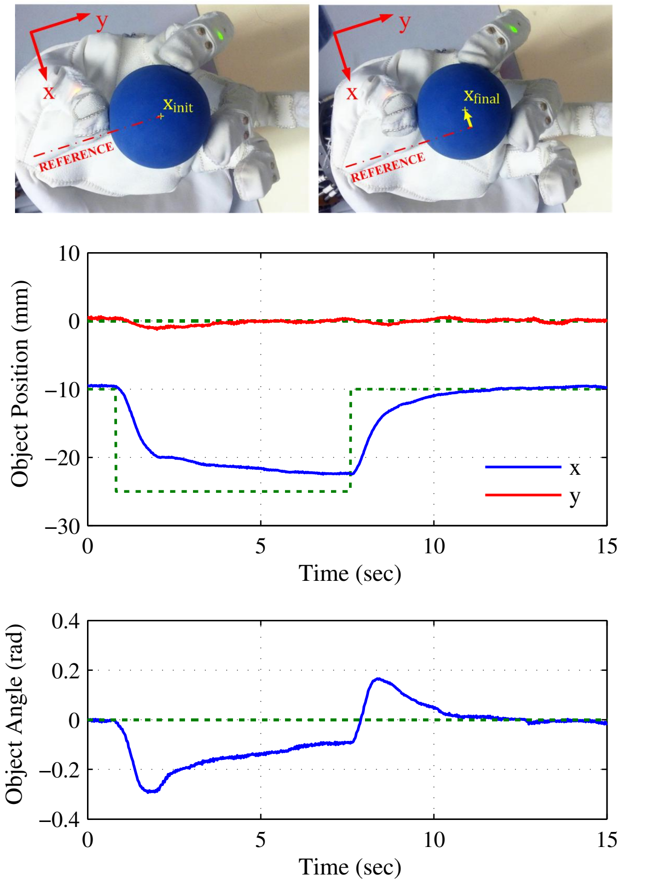

Fig. 4. The R2 hand translating the ball laterally, given a commanded x-direction step input from $x = -10\ mm$ to $x = -25\ mm$.

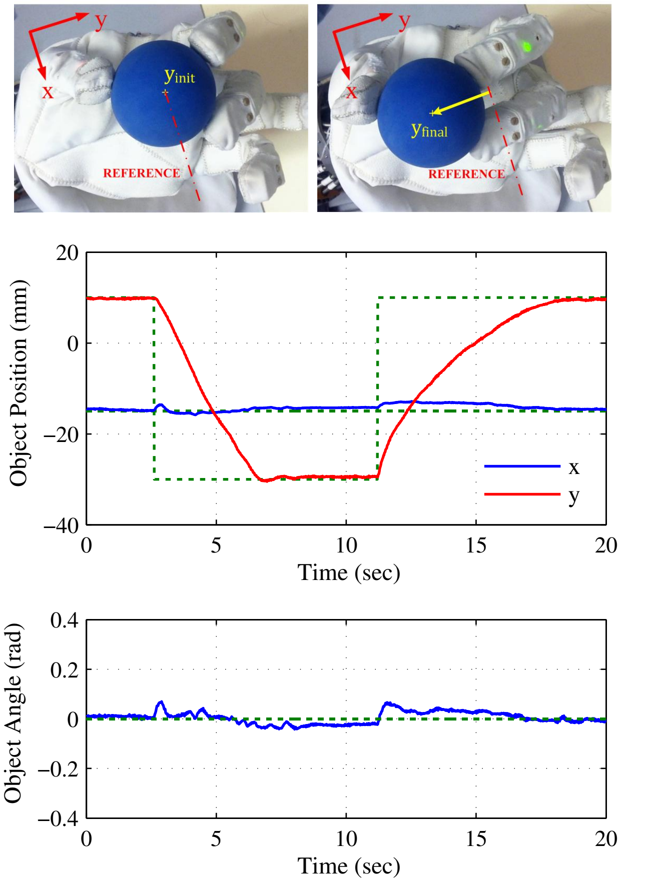

Fig. 5. The R2 hand translating the ball vertically, given a commanded y-direction step input from $y = 10\ mm$ to $y = -30\ mm$.

forces in Fig. 6(d) are defined as the projected component of fingertip forces passing through the center of the ball, producing a normal gripping force. There are intervals when the internal thumb force drops below the threshold; this occurs because the disturbance is in reality being applied to the thumb and not directly to the ball, skewing thumb force values in the negative direction. At all other times, the desired minimum grip force of $f_{grip,min} = 0.5$ is maintained. Note that the tension sensors have an error of 5-10% caused by friction and interactions between tendon conduits [7], which limits the controller's performance and precision.

V. Conclusions

In this paper we have presented a Cartesian stiffness control law for the fingers and thumb of the R2 hands and an object-level control for fine manipulation tasks. The Cartesian controller builds upon the existing joint-space controller with a number of novel additions and modifications. We developed a hybrid Cartesian and joint stiffness control law such that singularities are avoided in the primary fingers and distal joint stiffness is added in the thumb for full controllability. The proposed controller allows for an intuitive control of fingertip positions and forces using only tendon tension sensors as force feedback, and explicit control of key joint angles (primary finger yaw joints, thumb distal joints) that are important in manipulation tasks for ensuring good contact areas and stable grasps. We then implemented this controller as part of a higher-level object controller for multiple fingers performing fine manipulation tasks. The fingertip positions were used to define a virtual object position on a 2-D plane above the palm, which was subsequently used to implement an object stiffness control law. This controller was implemented on the R2 hand, and experimental results demonstrate stable grasping, smooth object motions, and robustness against disturbances.

The requirements on the R2 hand are broad and challenging. Various fine manipulation tasks are required on the ISS, such as pulling and turning knobs on a task board and using space tools (see Fig. 1). This paper introduces novel control strategies that take full advantage of R2's well-designed hardware and sensing capabilities. Future work will include the utilization of 6-DOF force/torque sensors located in the fingertips to allow for more precise control of fingertip forces, faster movements, and expansion of the object-level controller to 3-D motions.

References

[1] A. Bicchi, "Hands for dexterous manipulation and robust grasping: A difficult road toward simplicity," *IEEE Transactions on Robotics and Automation*, vol. 16, pp. 652–662, 2000.

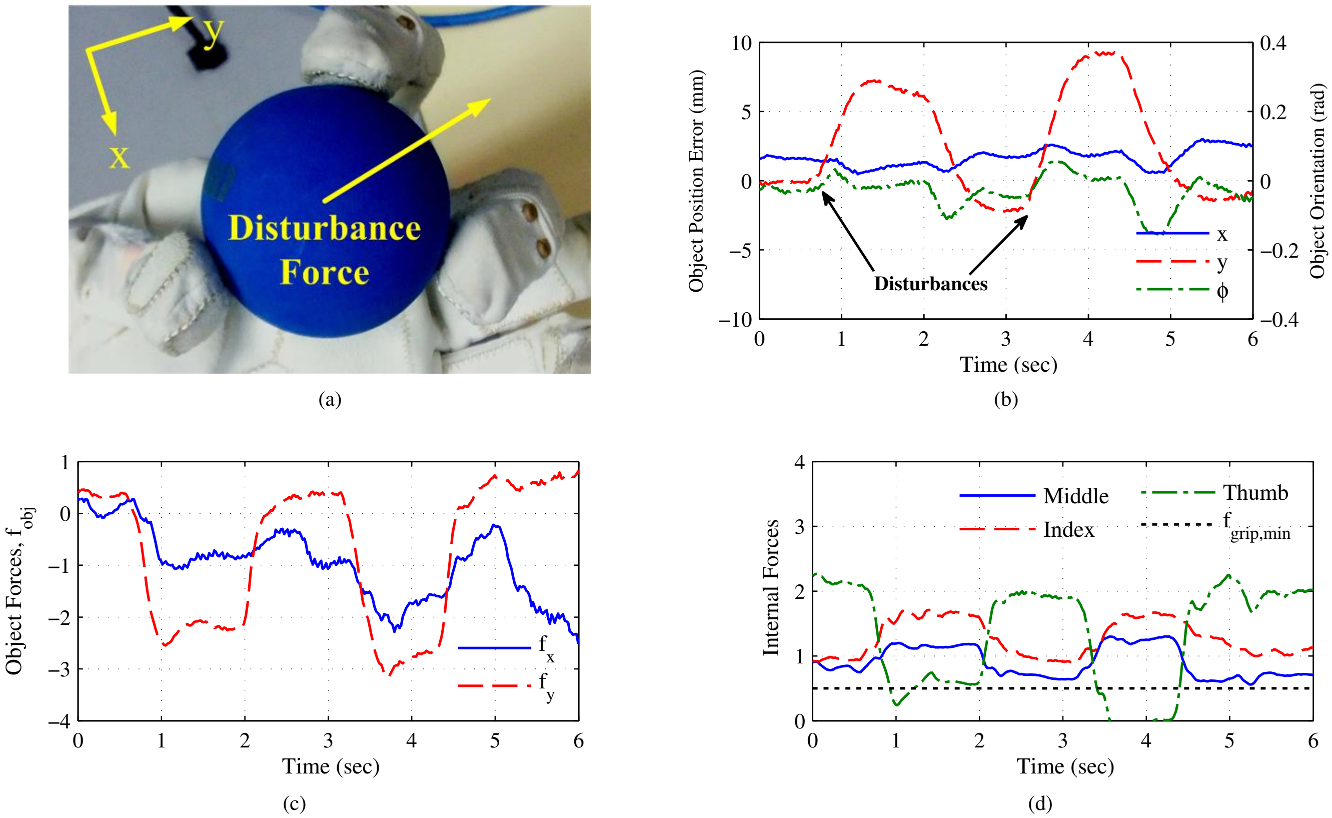

Fig. 6. The R2 hand attempting to maintain the a set object position given a disturbance, as shown in (a). The object's virtual position and orientation response through two disturbance impulses is shown in (b), while (c) and (d) shows the resulting object forces $(f_{obj,x}, f_{obj,y})$ and internal forces being exerted on the object by the fingertips.

[2] M. Grebenstein, M. Chalon, W. Friedl, S. Haddadin, T. Wimböck, G. Hirzinger, and R. Siegwart, "The hand of the DLR hand arm system: Designed for interaction," *The International Journal of Robotics Research*, vol. 31, no. 13, pp. 1531–1555, 2012.

[3] A. D. Deshpande, Z. Xu, M. J. V. Weghe, B. H. Brown, J. Ko, L. Y. Chang, D. D. Wilkinson, S. M. Bidic, and Y. Matsuoka, "Mechanisms of the anatomically correct testbed hand," 2011.

[4] J. K. Salisbury, "Active stiffness control of a manipulator in cartesian coordinates," in *IEEE Conference on Decision and Control including the Symposium on Adaptive Processes*, vol. 19. IEEE, 1980, pp. 95–100.

[5] N. Hogan, "Impedance control: An approach to manipulation," *Journal of Dynamic Systems, Measurement, and Control*, vol. 107, pp. 1–24, 1985.

[6] L. Biagiotti, H. Liu, G. Hirzinger, and C. Melchiorri, "Cartesian impedance control for dexterous manipulation," in *IEEE/RSJ International Conference on Intelligent Robots and Systems (IROS)*, vol. 4. IEEE, 2003, pp. 3270–3275.

[7] L. B. Bridgwater, C. Ihrke, M. A. Diftler, M. E. Abdallah, N. A. Radford, J. Rogers, S. Yayathi, R. S. Askew, and D. M. Linn, "The Robonaut 2 hand-designed to do work with tools," in *IEEE International Conference on Robotics and Automation (ICRA)*. IEEE, 2012, pp. 3425–3430.

[8] M. Abdallah, R. Platt, C. Wampler, and B. Hargrave, "Applied joint-space torque and stiffness control of tendon-driven fingers," in *IEEE-RAS International Conference on Humanoid Robots (Humanoids)*. IEEE, 2010, pp. 74–79.

[9] Y.-T. Lee, H.-R. Choi, W.-K. Chung, and Y. Youm, "Stiffness control of a coupled tendon-driven robot hand," *Control Systems, IEEE*, vol. 14, no. 5, pp. 10–19, 1994.

[10] S. Arimoto, K. Tahara, J. Bae, and M. Yoshida, "A stability theory of a manifold: concurrent realization of grasp and orientation control of an object by a pair of robot fingers," *Robotica*, vol. 21, no. 2, pp. 163–178, 2003.

[11] S. Arimoto and M. Yoshida, "Modeling and control of three-dimensional grasping by a pair of robot fingers," *SICE Journal of Control, Measurement, and System Integration*, vol. 1, pp. 2–11, 2011.

[12] M. Gabiccini, M. Branchetti, and A. Bicchi, "Dynamic optimization of tendon tensions in biomorphically designed hands with rolling constraints," in *IEEE International Conference on Robotics and Automation (ICRA)*. IEEE, 2011, pp. 2698–2704.

[13] S. Schneider and R. Cannon Jr, "Object impedance control for cooperative manipulation: Theory and experimental results," *IEEE Transactions on Robotics and Automation*, vol. 8, no. 3, pp. 383–394, 1992.

[14] D. Prattichizzo, M. Malvezzi, M. Aggravi, and T. Wimbock, "Object motion-decoupled internal force control for a compliant multifingered hand," in *IEEE International Conference on Robotics and Automation (ICRA)*. IEEE, 2012, pp. 1508–1513.

[15] M. Malvezzi and D. Prattichizzo, "Internal force control with no object motion in compliant robotic grasps," in *IEEE/RSJ International Conference on Intelligent Robots and Systems (IROS)*. IEEE, 2011, pp. 1008–1014.

[16] T. Wimboeck, C. Ott, and G. Hirzinger, "Passivity-based object-level impedance control for a multifingered hand," in *IEEE/RSJ International Conference on Intelligent Robots and Systems (IROS)*, 2006, pp. 4621–4627.

[17] T. Wimböck, C. Ott, A. Albu-Schäffer, and G. Hirzinger, "Comparison of object-level grasp controllers for dynamic dexterous manipulation," *The International Journal of Robotics Research*, vol. 31, no. 1, pp. 3–23, 2012.

[18] E. R. Kandel, J. H. Schwartz, T. M. Jessell, S. A. Siegelbaum, and A. J. Hudspeth, Eds., *Principles of Neural Science*. McGraw-Hill Professional, 2012.